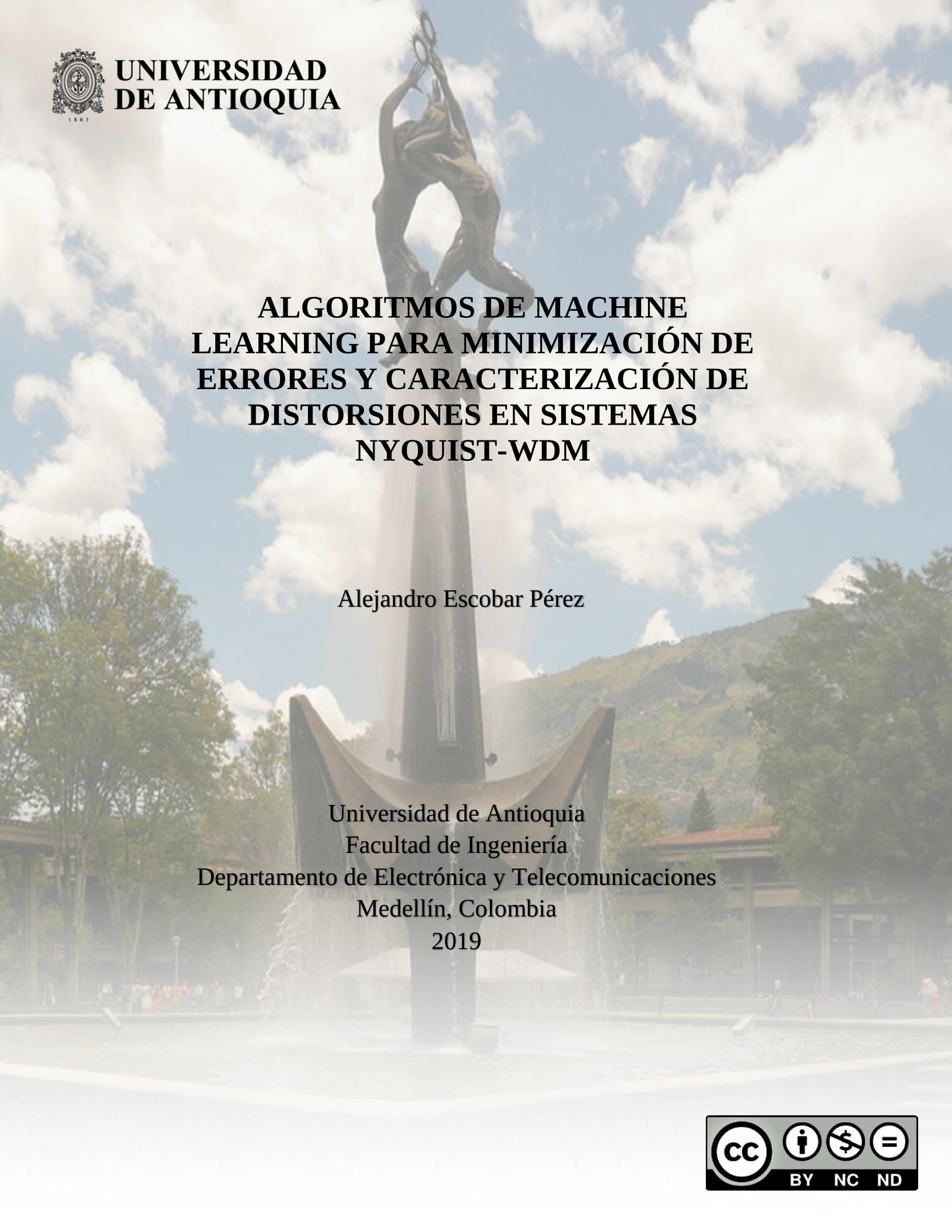

UNIVERSIDAD DE ANTIOQUIA

ALGORITMOS DE MACHINE LEARNING PARA MINIMIZACIÓN DE ERRORES Y CARACTERIZACIÓN DE DISTORSIONES EN SISTEMAS NYQUIST-WDM

Alejandro Escobar Pérez

Universidad de Antioquia
Facultad de Ingeniería
Departamento de Electrónica y Telecomunicaciones
Medellín, Colombia
2019

Resumen

La necesidad de incrementar la velocidad de transmisión en los sistemas de comunicaciones ópticas debido al aumento en la demanda de datos por parte de los usuarios finales ha dado el surgimiento al paradigma conocido como redes ópticas elásticas. Estas redes, principalmente basadas en sistemas Nyquist-WDM, permiten el aumento de la eficiencia espectral resultando en mayor capacidad de transmisión. Sin embargo, el espaciamiento reducido entre los canales ópticos generados en estas redes, resulta en Interferencia Inter-Canal (ICI, del inglés *Inter-Channel Interference*). Este fenómeno se ha modelado como ruido Gaussiano. Por lo tanto, su mitigación y diagnóstico es una tarea compleja que es actualmente investigado. Técnicas basadas en algoritmos de aprendizaje automático (en inglés *Machine Learning*) han surgido como herramientas para monitoreo y mitigación de diferentes efectos que ocurren en sistemas de comunicaciones ópticas. En este trabajo de grado, se proponen 2 técnicas para diagnosticar la ICI. La primera técnica se basa en el algoritmo Fuzzy *c*-Means (FCM) junto con el algoritmo *K*-Nearest Neighbors (KNN) para estimar el porcentaje de traslape espectral. La segunda técnica se basa en el cálculo de histogramas de la señal en fase y cuadratura, y posterior estimación de traslape espectral apoyado del algoritmo KNN. Se lograron porcentajes de acierto de hasta 92% y 70%, respectivamente para cada técnica. Para mitigación de la ICI, se aplicaron los algoritmos *k*-Means y KNN, donde, en escenarios simulados se alcanzaron ganancias de hasta 2 dB en términos de señal a ruido óptico (OSNR, del inglés *Optical Signal to Noise Ratio*) y para escenarios experimentales, se obtuvieron ganancias de hasta 1.3 dB. Finalmente, se pudo concluir que técnicas basadas en algoritmos de aprendizaje automático podrán ser útiles tanto para monitoreo de red, por ejemplo, para controlar frecuencias de las portadoras en futuros sistemas Nyquist-WDM, así como para la mitigación de diferentes fenómenos lineales y no lineales que afectan la transmisión de señales ópticas.

Abstract

The increment of data demand by end users creates the need of higher transmission rates in the current optical networks. The paradigm of elastic optical networks based on Nyquist-WDM systems seems to be a convenient solution where the spectral efficiency is increased. However, the low spectral spacing between channels generates Inter-Channel Interference (ICI), effect modeled as Gaussian noise. Therefore, monitoring, diagnostic and mitigation of ICI is an important issue to be researched. Moreover, Machine Learning (ML)-based techniques promise improvement of traditional monitoring and mitigation of different effects in optical communications. Thus, in this work, two ML techniques were proposed for ICI diagnostic. The first one is based on Fuzzy *c*-Means (FCM) in joint with *K*-Nearest Neighbors (KNN) algorithm, for channel overlapping estimation. The second one is based on the calculation of histograms using the In-Phase and Quadrature signal components with KNN estimation. Results showed an accuracy up to 92% and 70%, respectively. For ICI mitigation, the algorithms *k*-Means and KNN were applied for digital demodulation. In simulated scenarios, gains up to 2 dB of OSNR were obtained, while in experimental scenarios, gains up to 1.3 dB were achieved. Finally, these ML-based techniques could be implemented to improve monitoring techniques, for example, to control laser frequencies in future terabit gridless optical multicarrier systems and for mitigation of linear and non-linear fiber optical effects.

1. Introduction

Advances in multicarrier optical transmission systems rely on digital signal processing (DSP)-based coherent receivers have come out in the last years for increasing the transmission speed in optical fiber networks due to the ever-growing demand of data by end users [1]. Foreseeing these optical multicarrier scenarios, a flexible grid with a granularity of 12.5 GHz was recommended by the ITU-T for wavelength division multiplexing (WDM) in contradistinction to the spectral fixed-grid of 50 GHz, to achieve higher data rate transmitting multiple channels as a single entity (superchannels) with a reduced channel spacing [2]. To further increase the spectral efficiency (SE), those channels (subcarriers), can be spectrally generated very close or even overlapped, resulting in interchanel-channel interference (ICI). This ICI, due to optical spectral overlapping, can be mitigated by several techniques using the information of the adjacent channels, such as: multiple inputs multiple outputs (MIMO)-based equalizers [3]–[6], bit-coding among subcarriers (i.e. Han-Kobayashi and Dirty-Paper coding [7] and bit-multiplexing including hard-decision FEC [8]) or in optical domain by means of wave mixing approaches [9], [10]. However, the flexibility granted by the future gridless scenarios with reconfigurable optical add/drop multiplexers (ROADM) at different nodes, will not guarantee that a channel affected by ICI could be equalized using information of adjacent channels [1]. Fig. 1 shows a gridless scenario where the channels are added and dropped out at different nodes such that, a channel can be affected by several adjacent channels during its transmission, and the information of such adjacent channels are not available at the end node [11], [12].

Since ICI has been modeled as linear noise-like distortion [13], [14], estimation, monitoring and mitigation of ICI is an important and challenging issue in future gridless scenarios [15], [16]. Nevertheless, when channels are overlapped the data symbols belonging to a specific channel can interact among adjacent channels, resulting in non-symmetric deviation and/or redistribution of symbols seen in short time windows in a constellation diagram [17] (see Fig. 2). Detection of nonsymmetrical boundaries or thresholds in constellation diagrams have been performed by

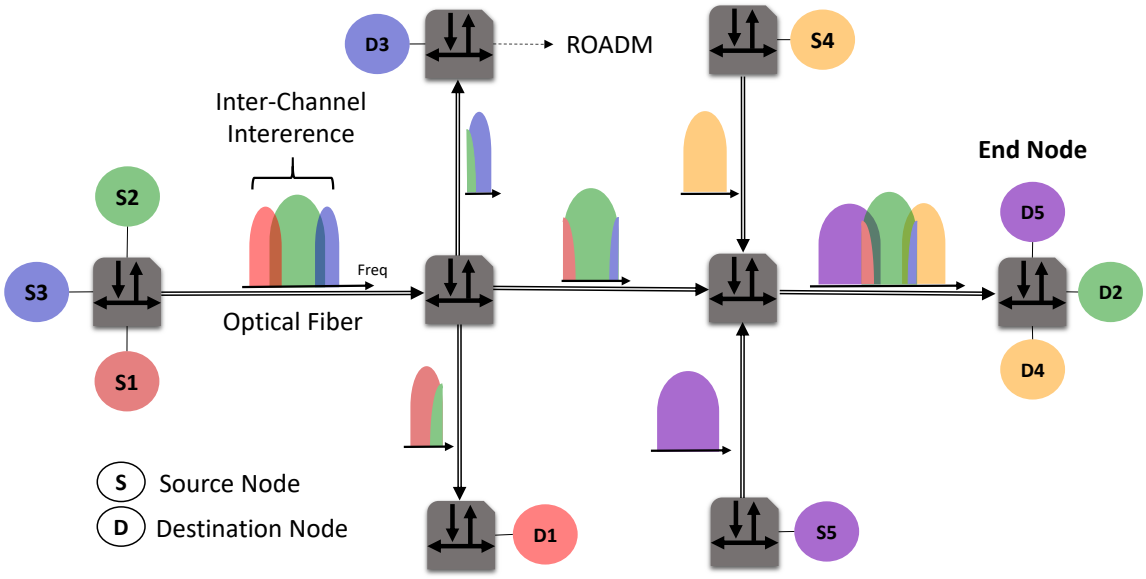

Fig. 1. Inter-Channel Interference in future Gridless WDM systems due the add-drop process of channels.

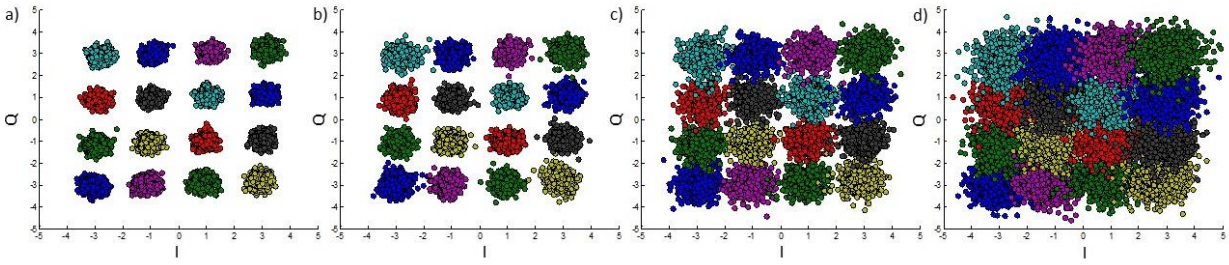

Fig. 2. 16QAM Spectral Overlapping Distortions for 36.3 dB of OSNR in a 17.6 GBds transmission. a) Single Channel. b) 6.8% Spectral Overlapping. c) 18% d) 24%.

Machine Learning (ML) techniques [18]–[20]. Besides, traditional monitoring and demodulation methods has been improved by some of these techniques based on ML algorithms [16], [17], [20]–[24].

Thereby, in this work we propose two methods for spectral overlapping estimation using ML based on constellation diagram analysis. The first one is based on Fuzzy c-Means (FCM) combined with *k*-Nearest Neighbors (KNN), taking advantage of the partition matrix of membership degrees given by the FCM and the cluster centroid updating of the received symbols in a constellation diagram. The results will be submitted to scientific international journal. The second method estimates channel overlapping using KNN based on histograms of the In-Phase and Quadrature components of received symbols frames.

Effectiveness of both methods are experimentally verified in a 3×16 Gbaud 16QAM Nyquist WDM system, with significant ICI due to reduced channel spacing. The proposal takes advantages of using ML algorithms which can be adapted to different scenarios when spectral overlapping may occur. Besides, the ICI tracking is performed using short frames of only 10k symbols, viable for practical monitoring tools.

Besides, two demodulation techniques based on ML were applied to 100k symbols frames affected by ICI. *k*-Means and KNN were first applied to simulated Nyquist-WDM single channel scenario in VPIDesignSuite® software, reducing fiber non-linear effects by both techniques. The simulation results were presented and published in the proceedings of the Colombian Conference on Communications and Computing 2019 (COLCOM) congress organized by the IEEE [25]. Furthermore, both methods were applied to experimental frames of 100k symbols reducing ICI, reaching up a low-length training stage by KNN and gains by both algorithms, results obtained were presented and published in the proceedings of the Advanced Photonics Congress 2019 organized by the OSA [26].

The remainder of this work is organized as follows: in section 2, the respective monitoring methods are explained and detailed, demodulation methods are explained in section 3, simulated and experimental setup are described in section 4, results and discussion are given in section 5, finishing with conclusions in section 6.

2. Optical spectral overlapping estimation based on Machine Learning

2.1. Method based on Fuzzy *c*-Means and KNN

Fuzzy c-Means so called the fuzzy version of well-known *k*-Means algorithm is a clustering technique with indirect classification that gives to each analyzed data a probability to be part to every single cluster [27]. In a constellation diagram analysis for m-QAM modulation formats, every ideal position of symbols is positioned as starting cluster centroid, when a received symbol is analyzed, the membership degree to every cluster is calculated based on distance to each centroid, minimizing the function (1) where N is the number of clusters, K is total received symbols, μ is the vector for closest clusters centroid and r is the normalization matrix.

$$J = \sum_{n=1}^{N}\sum_{k=1}^{K} r_{nk} \left\|(x_n - \mu_j)\right\|^2 \qquad (1)$$

For example, in a 16-QAM, every received symbol would have 16 membership degrees (one for each modulation symbol) as Fig. 3a shows, therefore, the classification results in a partition matrix of dimensions $16 \times L$ (where L the total received symbols) with elements that are numbers from 0 to 1, hence, after every membership degrees calculation, centroid position is updated by the mean of the closest symbols to every centroid.

In a transmission channel with ICI, it is evidenced that the closest cluster is not always the correct one, it results in scenarios like Fig. 3b shows, where while noise increases, the belonging symbols suffers membership degree reduction. In the classification for demodulation, it is assigned to each

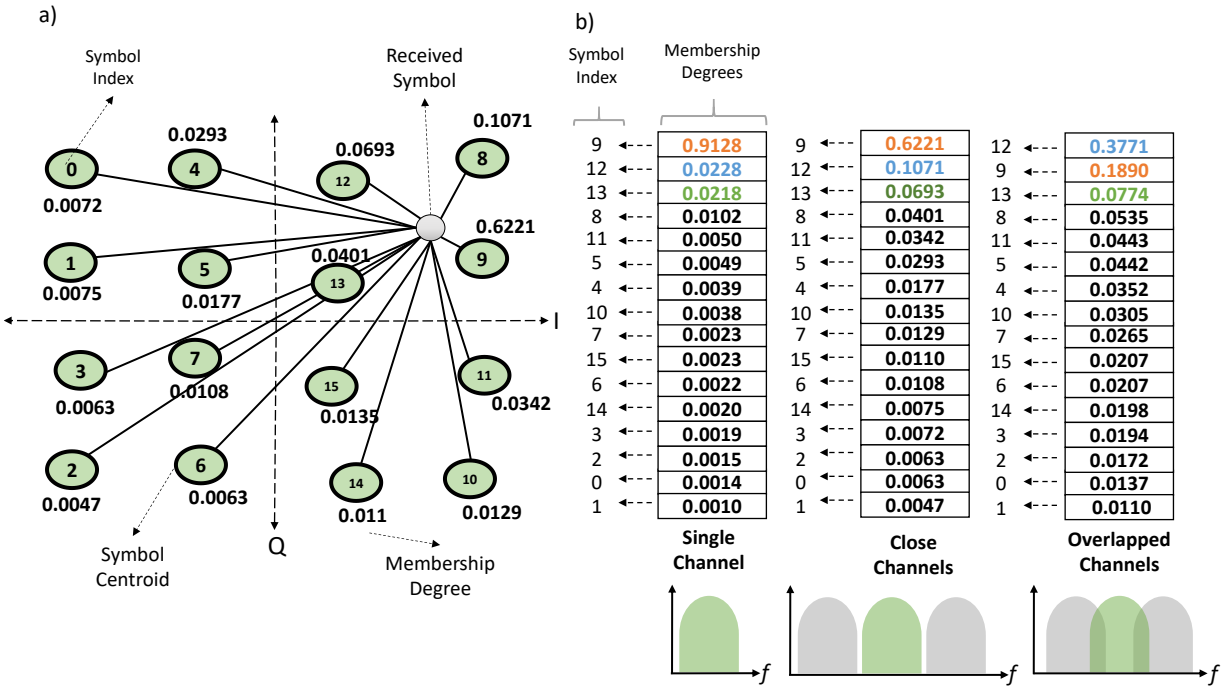

Fig 3. a) Fuzzy c-Means Classification for received symbol in a 16-QAM modulation format with close channels scenario. b) Membership degrees for different spectral overlapping for a single received symbol at a 36.3 dB of OSNR transmission.

received symbol, the cluster with the highest membership degree, creating demodulation errors. Hence, it is verified that having a highest membership degree election of symbol for demodulation, FCM shows almost exact bit error rate (BER) performance as *k*-means does [25].
Using the given FCM matrix, the membership degrees are sorted in descending order and analyzed the belonging symbol position. It is counted how many symbols with the highest membership degree were the correct ones, and the same is done for the second, third, fourth-highest and so on up to the 16th highest (last) membership degree.

Tables 1 to 3 shows the number of symbols that its closest centroid (1st) matches to the correct modulation value or second (2nd) and so on according to the sorted FCM matrix, for some spectral overlapping scenarios (including single channel), at 36.3 dB and 14.3 dB, respectively.

Ch. Overlapping / Centroid Closeness	**1°**	**2°**	**3°**	**4°**	**5°**	**6°**	**7°**	**8°**	**9°**	**10°**
Single Channel	100.000	0	0	0	0	0	0	0	0	0
0%	99963	35	2	0	0	0	0	0	0	0
18%	98777	1163	51	9	0	0	0	0	0	0
30%	82890	12712	2651	1362	233	117	29	4	2	0

Table 1. FCM classification for 36.3 dB of OSNR.

Ch. Overlapping / Centroid Closeness	**1°**	**2°**	**3°**	**4°**	**5°**	**6°**	**7°**	**8°**	**9°**	**10°**
Single Channel	99261	734	4	1	0	0	0	0	0	0
0%	98006	1932	52	10	0	0	0	0	0	0
18%	94702	4843	328	119	5	2	1	0	0	0
30%	75822	16851	4225	2111	586	272	84	27	15	3

Table 2. FCM classification for 19.3 dB of OSNR.

Ch. Overlapping / Centroid Closeness	**1°**	**2°**	**3°**	**4°**	**5°**	**6°**	**7°**	**8°**	**9°**	**10°**
Single Channel	85034	12679	1673	571	32	9	2	0	0	0
0%	81606	14744	2492	991	106	47	11	3	0	0
18%	76549	17488	3701	1662	376	154	56	12	1	1

Table 3. FCM classification for 14.3 dB of OSNR.

Single channel scenario at 36.3 dB of OSNR (considered as low-noise) in Table 1, shows that all the 100k symbols belongs to the first membership degree. While in Table 3 where OSNR is 14.3 dB, the first membership degree counts on 85k symbols and 12.679 symbols were correct at the second closest centroid. Moreover, the penalty created by the low OSNR is compared to spectral overlapping, in Table 1, the 30% channel overlapping scenario gave 12.712 at the second choice, almost the same as single channel with 14.3 dB of OSNR.
After the process carried out with the FCM algorithm, the resulted counting vectors are taken as inputs to the KNN algorithm to estimate the percentage of spectral overlapping. The election of KNN parameters was performed varying the number of neighbors and the length of training data

to obtain the best accuracy in all cases. The Fig. 4a shows that there is an accuracy variation lower than 6% between using only 25% or more than 90% of the symbols for training. Fig. 4b shows that a good value of neighbors is 3 for all cases.

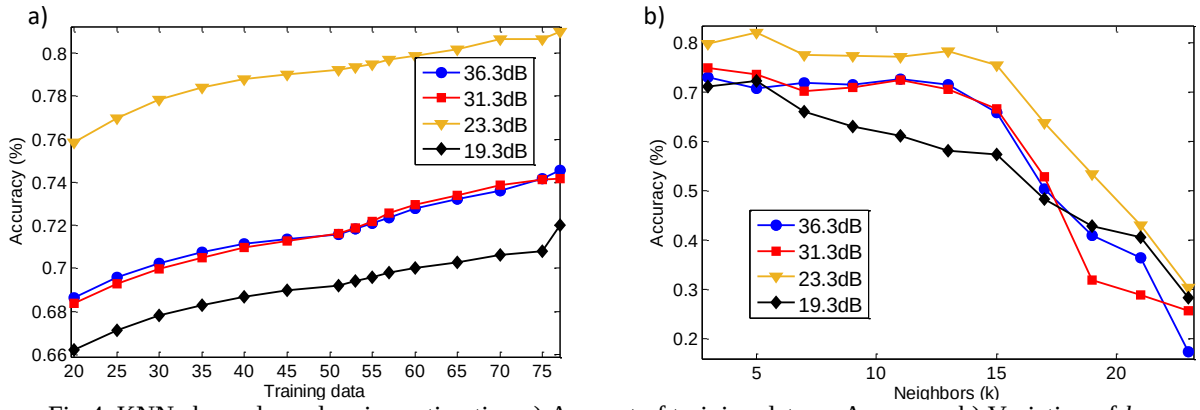

Fig 4. KNN channel overlapping estimation a) Amount of training data vs Accuracy. b) Variation of *k* vs Accuracy.

2.2. Method based on KNN applied to Histograms

The second channel overlapping estimation method is based on analysis given by histograms of both In-Phase and Quadrature values of symbols of frames of 10k. The histograms are constructed following 2 parameters, first one are the *bins which* are the total number of slots where In-Phase and Quadrature range values are divided. For example, if the *bins* value of an ideal 16-QAM constellation (see orange dots in Fig. 5a) is 10, the range -3 to 3 will give a bin slot each 0.6 units. The second one are the *counts*, that are equivalent to the total of symbols that "fall" into each bin slot, for example, in ideal 16-QAM, all the symbols with an In-Phase value of -3, will "fall" into the bin around -3. For an overall view, Fig. 5a shows a constellation diagram of a frame of 10k symbols affected by a 12.5% channel overlapping at 19.3 dB of OSNR with its respective In-Phase histogram in Fig. 5b.

It is noticeable that the *counts* at the ideal 16-QAM symbols positions, give maximum values. Therefore, respective maximum and minimum *counts* values of both In-Phase and Quadrature components of frames of 10k symbols are given as features to KNN algorithm where an estimation

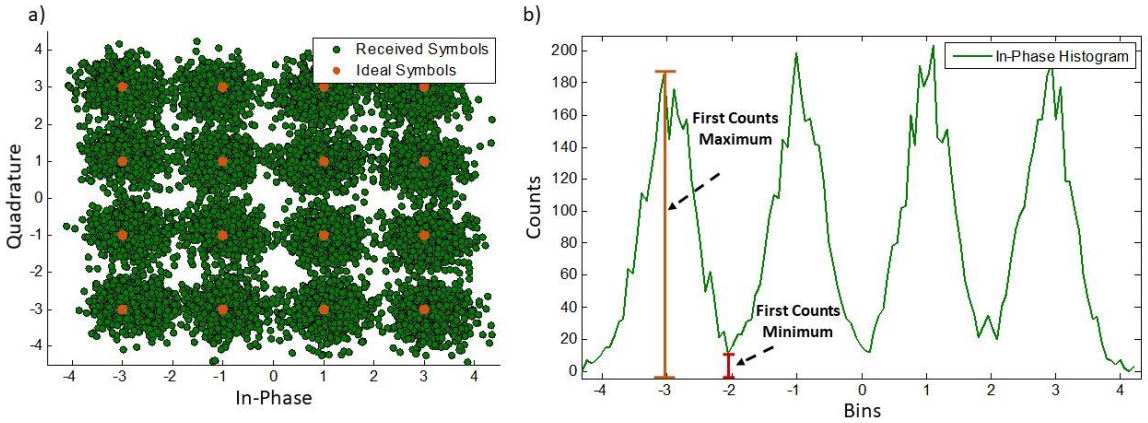

Fig. 5. a) 16-QAM constellation affected by 12.5% channel overlapping at 19.3 dB of OSNR. b) In-Phase component histogram of 10k symbols frame affected by 12.5% channel overlapping at 19.3 dB of OSNR.

of channel overlapping is made. Table 4, shows the In-Phase component features contribution to the KNN algorithm. Additionally, Quadrature component and the OSNR of signal is given as features as well, resulting in a total of 17 features per frame.

1° Counts Minimum (In Phase)	2° Counts Minimum (In Phase)	3° Counts Minimum (In Phase)	1° Counts Maximum (In Phase)	2° Counts Maximum (In Phase)	3° Counts Maximum (In Phase)	4° Counts Maximum (In Phase)	Counts vector length

Table 4. Features extracted from In-Phase Component Histogram.

3. Machine Learning-based Demodulation

3.1. Demodulation based on K-Nearest Neighbors

KNN is a supervised Machine Learning algorithm that based on certain training data, classifies different classes of data. Applied to a constellation diagram analysis, each received symbol would have an In-Phase component and Quadrature one and must be part of a modulation number or *class* (0-15 for 16-QAM). Each received symbol is compared with k-nearest training data following the Euclidean distance (equation (2), where X_r is the received symbol and X_t is an arbitrary training symbol) according to its IQ values (see Fig 6).

$$d(X_r, X_t) = \sqrt{(I(X_r) - I(X_t))^2 + (Q(X_r) - Q(X_t))^2} \quad (2)$$

Classification is made by choosing the most common class value among those "*k*" chosen neighbors classes as Fig. 6 shows. The training data is composed by certain % of 81 different frames of 100.000 received symbols each one affected by various channel spacing that goes from

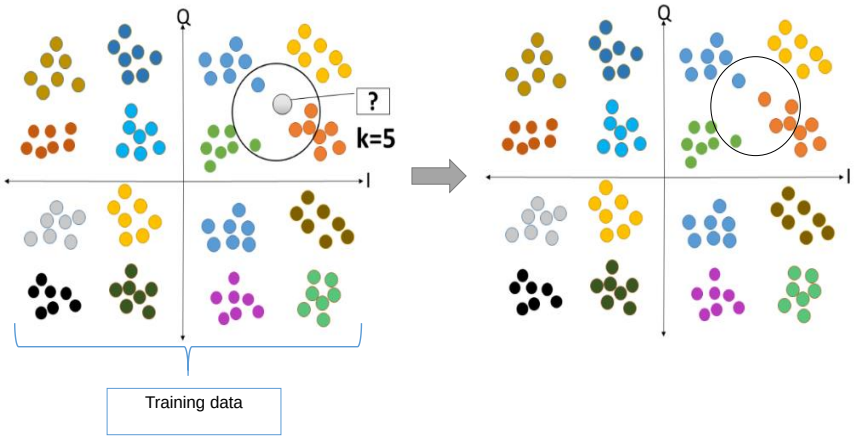

Fig. 6. KNN-based demodulator applied to a 16-QAM constellation.

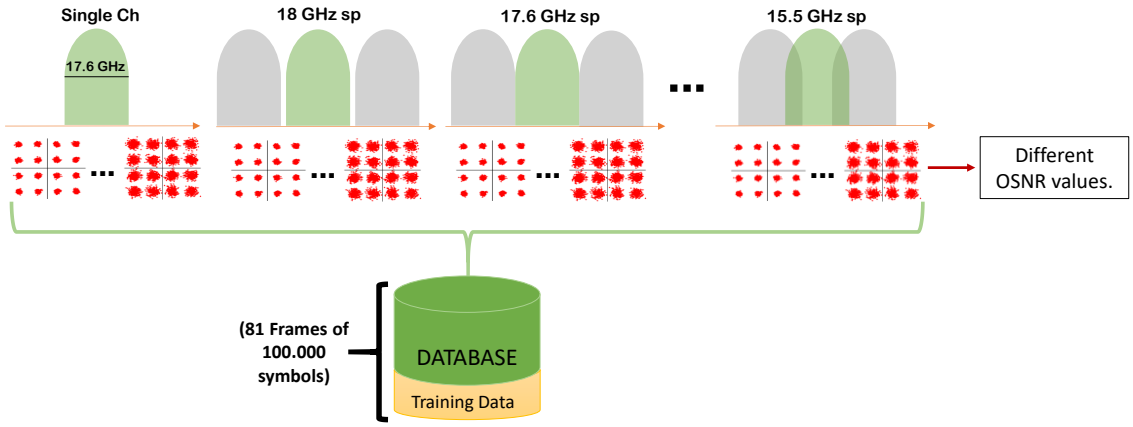

Fig. 7 Data Base configuration for training phase of KNN based demodulation.

a single channel to an overlapping of 30% stimulating ICI. Each scenario has different OSNR values that goes from 14.3 to 36.3 dB (see Fig. 7).

The choosing of *k* and percentage of training data was made by BER performance of demodulation following the curves at Fig. 8, where best BER values were achieved with *k*=15 and 3.240 symbols

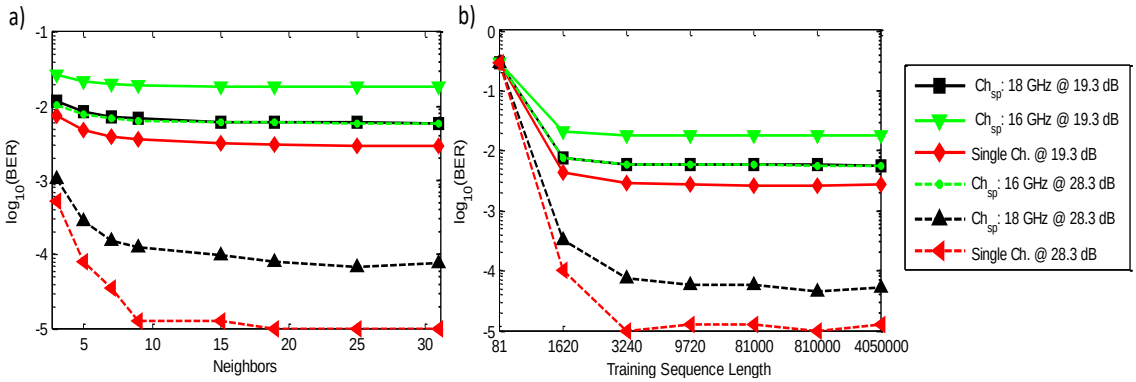

Fig. 8. 16QAM KNN-based demodulator a) Variation of *k* vs BER. b) Training Sequence Length vs BER.

for training (0.04% of each frame).

3.2. Demodulation based on *k*-Means

k-Means is a clustering classification algorithm with hard partitioning of data (Each symbol will be part of only one cluster) [27], that calculates centroids given a number of clusters (16 for 16-QAM). The initials values of centroids are given as the 16-QAM ideal constellation points. Classification starts by assigning closest centroid class to each received symbol as Fig 9 shows. The *k*-means algorithm is generalized by the equation (3) where *k* is the number of clusters and *n* is the total number of symbols that belong to the *j* cluster. Centroid's position is updated by the mean estimation of the classified data (4). Algorithm iterates until centroids do not change their position [28].

$$J = \sum_{j=1}^{k} \sum_{i=1}^{n} \left\| x_i^{(j)} - c_j \right\|^2 \quad (3) \qquad c_j = \frac{1}{n} \sum_{i=1}^{n} x_i^{(j)} \quad (4)$$

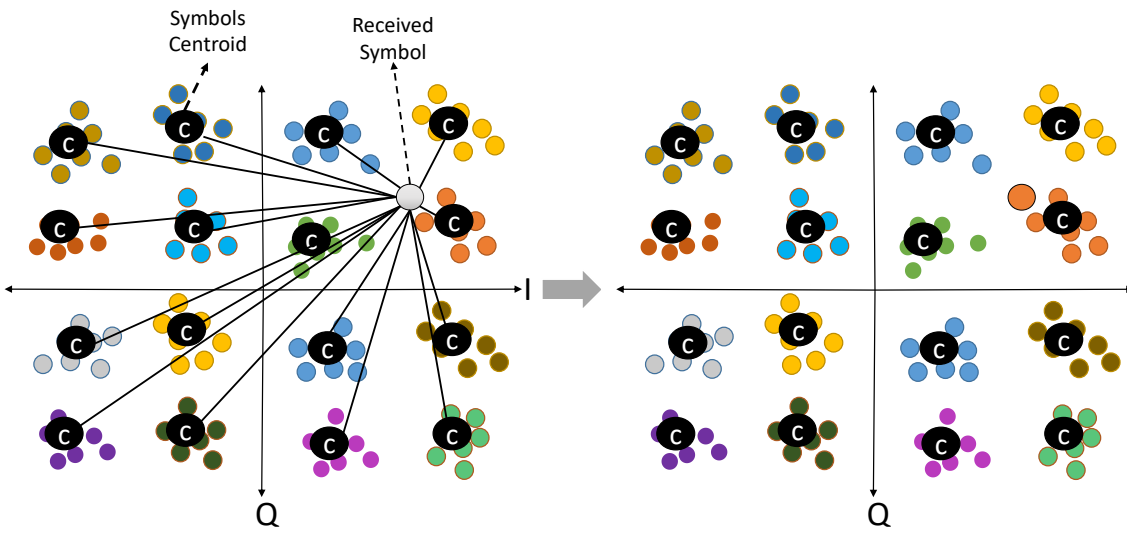

Fig. 9. 16-QAM *k*-Means based demodulation.

4. Simulation and Experimental Setup

4.1. Simulation Setup

Single carrier 16-QAM Nyquist coherent optical system at 32 Gbaud is modeled in VPIDesignSuite® (see Fig. 10). Pseudo Random Binary Sequence (PRBS) with length of 65536 bits is generated to be mapped in 16-QAM modulation format. Optical modulation is based on single drive MachZehnder Modulator (SD-MZM) including a continuous wave laser with different linewidth: 1 kHz, 25 kHz and 100 kHz. Launch power of 0 dBm and 9 dBm is guaranteed by ideal amplifier at the output of the optical transmitter. Signals are transmitted through single mode

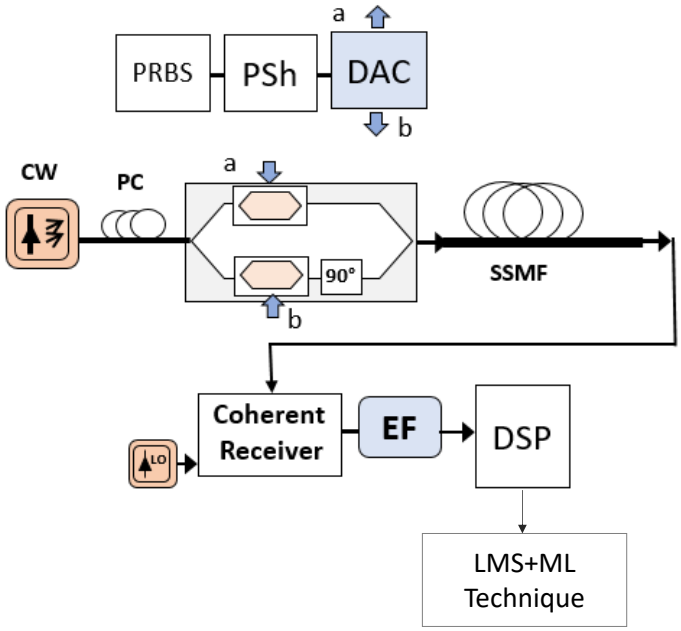

Fig 10. Simulation Setup of a 3x16 Gbaud 16QAM Nyquist-WDM.

nonlinear dispersive fiber (SMNDF) with distances up to 90 km. Optical noise is injected to yield and OSNR values from 0 to 25 dB. The optical coherent receiver includes a laser with the same configuration as the one used at the transmitter side. DSP module includes chromatic dispersion compensation, clock recovery and 5-taps LMS equalizer using a training sequence of only 300 symbols.

4.2. Experimental Setup

Fig. 11 shows the experimental setup based on three lasers arrangement with 100 kHz linewidth that are used to generate 3×16 Gbaud 16QAM Nyquist WDM system. The digital-analog converter (DAC) operates at 64 Gsamp/s and the center and side frequency channels are generated using different DACs to produce uncorrelated signals. Random bit sequences are mapped to generate 16-QAM symbols using a root raised cosine filter with roll-off factor of 0.1. Resulting in spectral widths of 17.6 GHz for each channel. The spacing between channels goes from single channel scenario to, 18 GHz (close channels), 17.6 GHz (0% overlap), 17 GHz (6.8% overlap), 16.5 GHz (12.5% overlap), 16 GHz (18% overlap), 15.5 GHz (24% overlap) and 15 GHz (30% overlap). Optical noise is aggregated to yield an OSNR of 14.3 to 36.3 dB. The receiver counts with a coherent wideband receiver of 35 GHz electrical bandwidth, then the signal is digitized by an 80 Gsamp/s real-time oscilloscope, finishing with an offline digital signal processing based on Matlab.

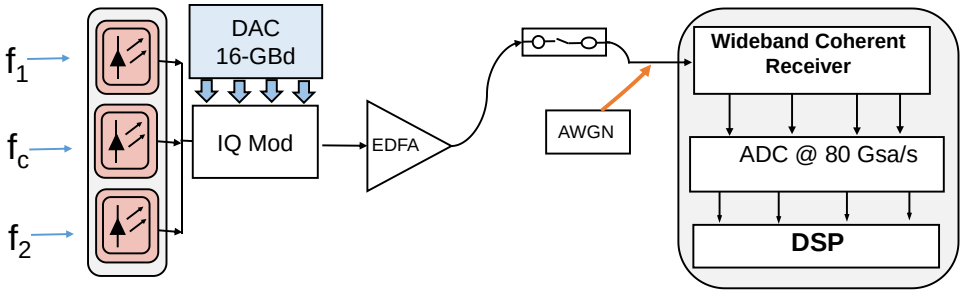

Fig 11. Experimental Setup of a 3x16 Gbaud 16QAM Nyquist-WDM.

5. Results and Discussions

5.1. Spectral Overlapping Estimation

5.1.1. Method based on FCM plus KNN

Channel overlapping estimation is made based on the analysis of the partition matrix given by FCM algorithm, comparing highest and non-highest membership degrees of a received symbol with its actual belonging symbol.

Results shown that at higher channel overlapping, higher is the amount of symbols where closest centroid to received symbols is not the correct one. Fig. 12 shows curves of percentage of actually correct symbols that are correct at the a) the highest, b) second highest and c) third highest, membership degree respectively according to FCM classification matrix vs OSNR for different channel spacing. Fig 12a shows that for a 30% of channel overlapping, the actual amount of symbols belonging to the highest membership level is 83% at 36.3 dB of OSNR. This means that ICI impairment gives an important error even when noise is minimum. Fig 12b shows the amount

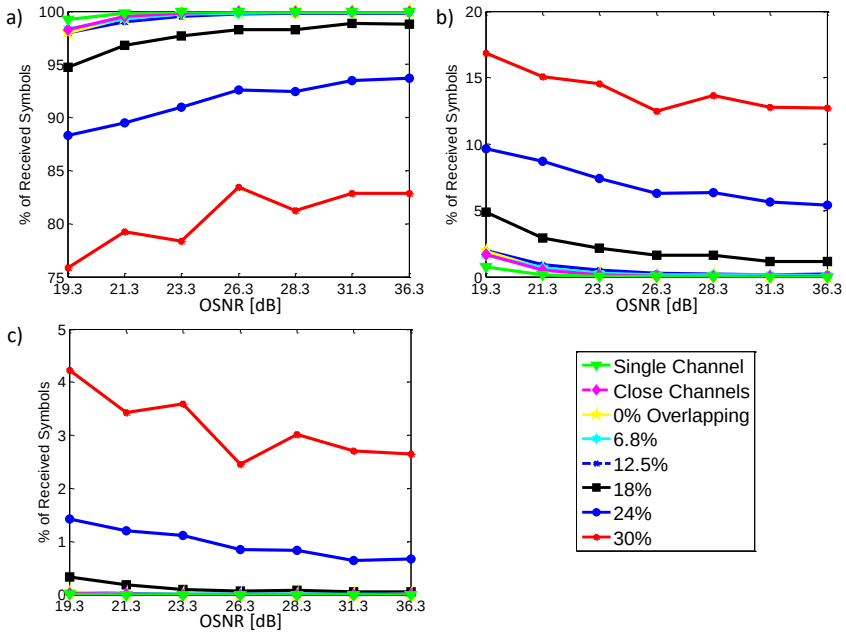

Fig 12. FCM Results a) Percentage of symbols where modulation symbol with first membership degree were correct ones. b) Second highest membership degree. c) Third highest.

of classified symbols where the belonging symbol had the second higher membership degree, besides, Fig 12c shows that almost 3% symbols are the third option as membership degree decrements at 30% channel overlapping and at 36.3 dB of OSNR.

The estimation results are based on percentage of accuracy using KNN. Spectral overlapping is predicted when resulted counting vectors of frames of 10k are inputs to KNN algorithm. Two possible monitoring scenarios are examined. The first one is seen in Fig. 13, where the OSNR is known by receiver and the spectral overlapping is estimated based on that value. It is noticed that when signals OSNR is high and channels experience low spectral overlapping e.g spacing of the same data rate, not overlapping at all (18 GHz spacing) or at single channel scenario, the resulted

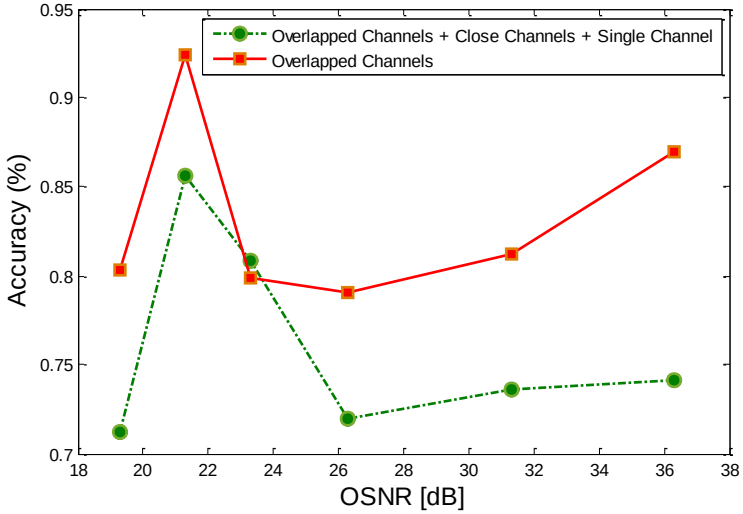

Fig 13. Channel-overlapping estimation accuracy based on FCM + KNN for every single OSNR values.

vectors due the FCM classification is almost the same (almost all the symbols belong to the closest centroid), nonetheless, when these scenarios are considered, estimation accuracy gives up to 85% at 21.3 dB of OSNR. Likewise, when these scenarios are not considered, 92.4% is obtained at 21.3 dB of OSNR. Hence, when OSNR is introduced as a feature into the KNN algorithm, accuracy percentage obtained was 76.23% and when single channel and close channels scenarios are not considered, the percentage obtained was 84%. The second monitoring scenario is when the signal OSNR is not known by the receiver, the KNN algorithm is trained and tested with only the counting vectors obtaining a 72% accuracy percentage when single channel and close channels scenario are not considered.

5.1.2. Method based on KNN applied to Histograms

The estimation results are based on percentage of accuracy using KNN. Channel overlapping is predicted when features of In-Phase and Quadrature histograms are inputs to KNN algorithm. This monitoring technique, brings two possible scenarios too. The first one is seen in Fig. 14, where the OSNR is known by receiver and the channel overlapping estimation is made based on that value. Likewise, as previous technique, histograms max-min values of counts given by single channel scenario and close channels scenarios (18 GHz spacing), are almost the same, thus, when these scenarios are considered, estimation accuracy presents 70% average accuracy. Likewise, when these scenarios are not considered, this average value is almost 80%. The second monitoring scenario (OSNR is not known by the receiver), shown a 66% accuracy percentage when single channel and close channels scenario are not considered.

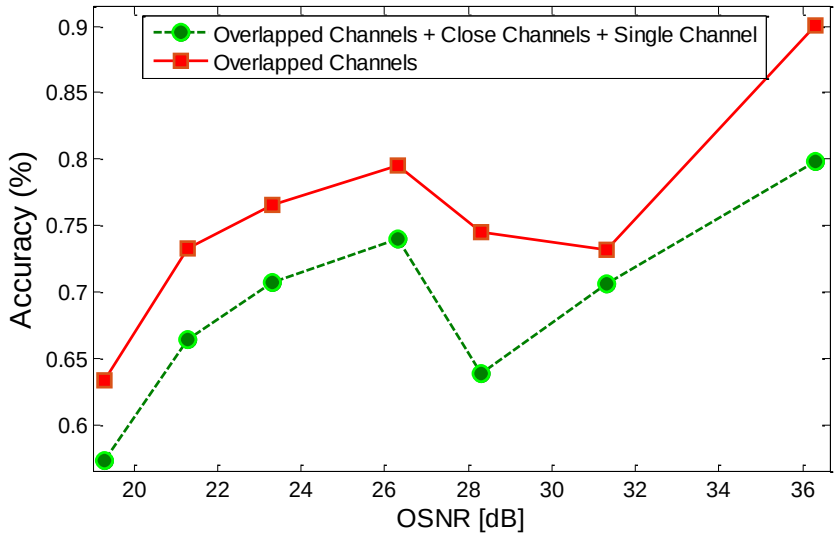

Fig 14. Channel-overlapping estimation accuracy based on Histograms + KNN for every single OSNR

5.2. Demodulation

5.2.1. Simulation Results

Our first step was the emulation of nonlinear noise-like distortions in Matlab. AWGN was added to yield OSNR values from 0 to 25 dB.

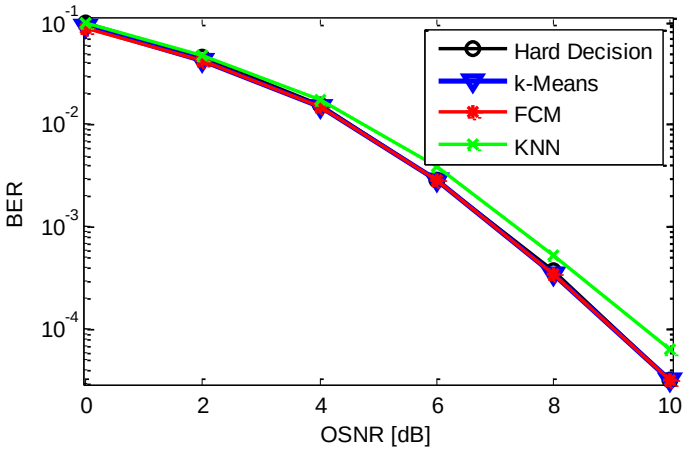

Fig 15. Channel-overlapping estimation accuracy based on Histograms + KNN for every single OSNR values.

Simulation of 16-QAM modulation format was introduced in such distortions emulation. LMS equalization was applied, and then, each ML technique were separately implemented after the equalizer module. BER vs ONSR curves are shown in Fig. 15. It is noticed that none of the three ML techniques improves the performance of LMS equalizer, this is because emulated effects in Matlab are totally mitigated by the LMS equalizer, leaving no errors to be corrected by the ML

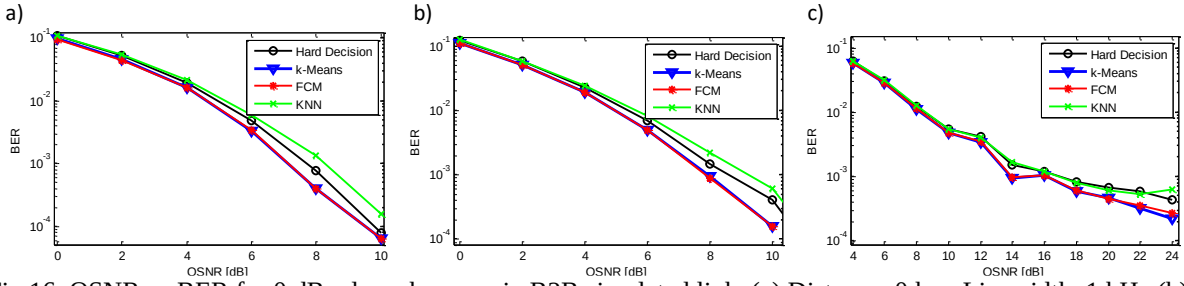

Fig 16. OSNR vs BER for 0 dBm launch power in B2B simulated link. (a) Distance: 0 km, Linewidth: 1 kHz (b) Distance: 0 km, Linewidth: 25 kHz (c) Distance: 0 km, Linewidth: 100 kHz.

techniques.

Fig. 16 shows BER performance vs OSNR for the coherent optical system, with launch power of 0 dBm, in back to back (B2B) scenario. Fig. 17 shows the cases of 25 km and 50 km of transmission distance using laser linewidth of 1 kHz, 25 kHz and 100 kHz. In Fig. 16a, it can be seen a sightly gain of ~ 0.2 dB by using both clustering techniques (*k*-Means and FCM). Due to it is B2B, the clustering corrects the impact of optical devices impairments, such as laser linewidth. In Fig. 17e, a BER value of 1×10^{-4} is reached at 14 dB after LMS equalization, while this same

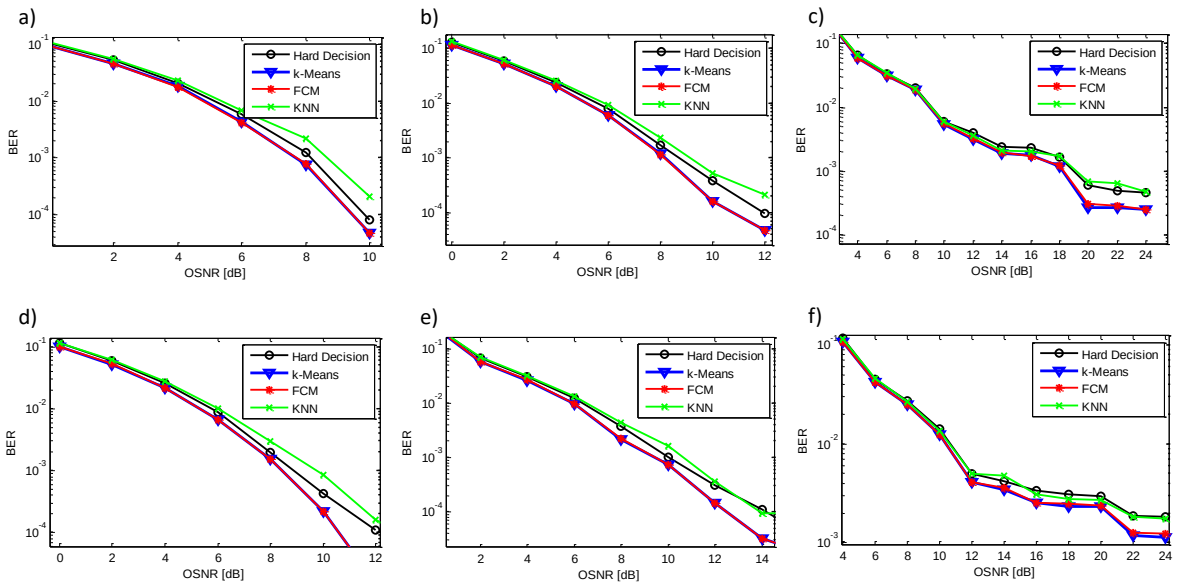

Fig 17. OSNR vs BER for 0 dBm launch power at 20 km and 50 km transmission distance. a) Distance: 20 km, Linewidth: 1 kHz. (b) Distance: 20 km, Linewidth: 25 kHz. (c) Distance: 20 km, Linewidth: 100 kHz. (d) Distance: 50 km, Linewidth: 1 kHz. (e) Distance: 50 km, Linewidth: 25 kHz. (f) Distance: 50 km, Linewidth: 100 kHz.

BER was reached by using clustering at 12 dB, being the highest gain achieved for cases with launch power of 0 dBm. For 100 kHz linewidth scenarios, results using clustering techniques shown a BER value around 2×10^{-4}after 20 dB for 20 km (see Fig. 17c) and 1.3×10^{-3} after 22 dB for 50 km of transmission distance (see Fig. 17f). Clustering techniques outperforms the BER in comparison with only electrical equalization, for all the cases simulated with a launch power of 0 dBm. KNN did not show better performance than LMS equalization. Actually, the performance was worst in scenarios of 1 kHz and 25 kHz of laser linewidth. Scenarios of 90 km transmission

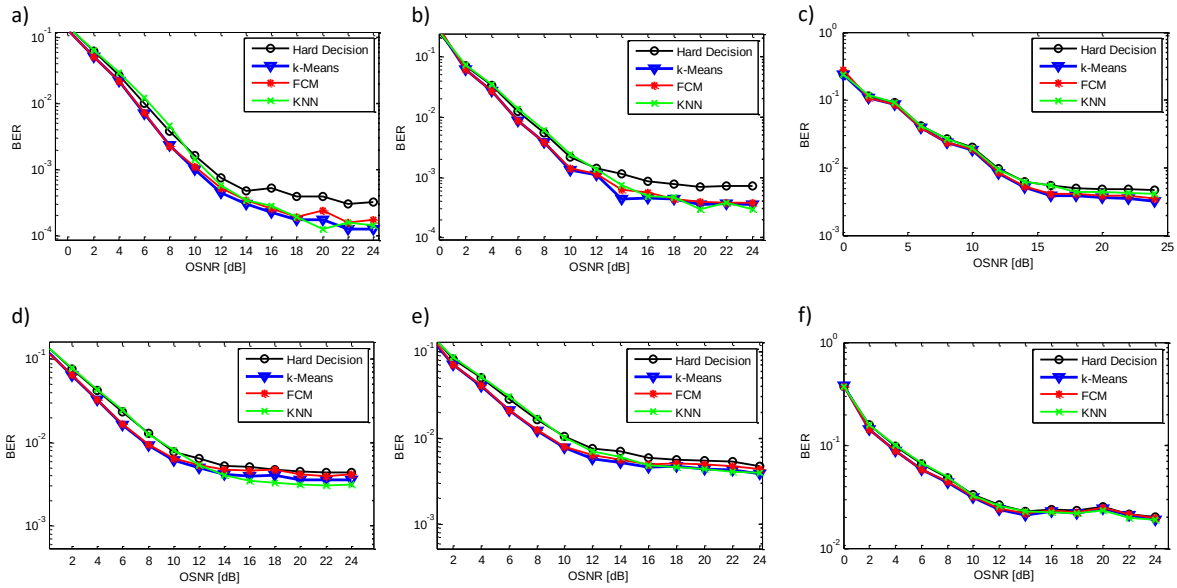

Fig 18. OSNR vs BER for 9 dBm launch power at 20 km and 50 km transmission distance. a) Distance: 20 km, Linewidth: 1 kHz. (b) Distance: 20 km, Linewidth: 25 kHz. (c) Distance: 20 km, Linewidth: 100 kHz. (d) Distance: 50 km, Linewidth: 1 kHz. (e) Distance: 50 km, Linewidth: 25 kHz. (f) Distance: 50 km, Linewidth: 100 kHz.

distance were simulated with laser linewidth of 25 kHz and 100 kHz, BER values of $1.7\times10^{-3}$and 1.9×10^{-2} were obtained by using clustering at 12 dB and 16 dB, respectively, keeping a gain of 2 dB compared with hard decision demodulation after LMS equalization.

Fig. 18 shows BER vs OSNR curves for cases with launch power of 9 dBm for 20 km and 50 km of transmission distance. Gain of 2 dB using clustering is obtained for 20 km of transmission distance with 25 kHz of laser linewidth at 12 dB of OSNR (see Fig. 18b). After 14 dB of OSNR, the BER obtained by using the adapted ML techniques, is higher than 3.1×10^{-3}, 5×10^{-3}, 1.6×10^{-2} for 1 kHz, 25 kHz and 100 kHz, respectively, at 50 km of transmission distance. For launch power of 9 dBm, KNN's performance is always better than LMS's in terms of BER, except when 100 kHz linewidth is used at 50 km transmission distance (see Fig. 18f), obtaining BER values higher than 1.8×10^{-2}.

5.2.2. Experimental Results

Fig. 19a to Fig. 19g show the performance of *k*-Means and KNN-based demodulation methods in terms of BER as a function of OSNR values for different channel spacing, including single channel. Results show better performance using the *k*-Means and KNN-based demodulation than the conventional demodulation based on hard decision. With both proposed demodulations, same gains up to 0.8 and 0.7 dB are reached for BER values at 7.6×10^{-3} and 1×10^{-2}, respectively for channel spacing of 16 GHz (see Fig. 19f). Moreover, it can be noticed that higher gains are obtained according channel spacing is reduced. It means the ICI effects are mitigated and this mitigation seems to be equally by both methods. For example, at channel spacing of 15.5 GHz (24% channel overlapping) in Fig. 19g, a gain of ~1.3 dB is obtained at BER of 3.1×10^{-2}, while for a channel spacing of 18 GHz (no overlap), gain is negligible (see Fig 1b). Besides, it is noticed that demodulation based on *k*-Means shows a slightly better performance than KNN at low interference scenarios.

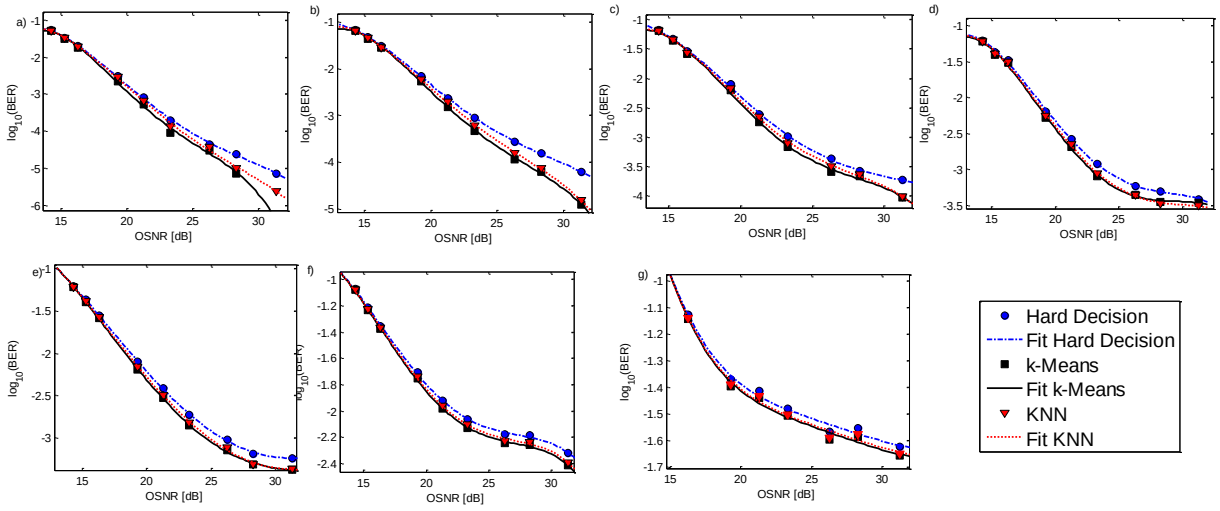

Fig. 19. BER vs OSNR for different spectral overlapping. a) Single Channel. b) Close Channels. c) 0% Channel Overlapping. d) 6.8%. e) 12.5%. f) 18%. g) 24%.
g) 15.5 GHz.

6. Conclusions

Two Machine Learning-based methods are experimentally applied to determine if any 16-QAM received signal has been affected by spectral overlapping in a 3×16 Gbaud Nyquist-WDM system. The methods were designed without information of adjacent channels and both methods give an estimation of optical spectral overlapping using frames of only 10k received symbols. First method, based on Fuzzy *c*-Means (FCM) and *K*-Nearest Neighbors (KNN) estimates the optical spectral overlapping based on resultant sorted counting vectors from the FCM matrix. Accuracy obtained reached up to 92% and 72% of accuracy with previous knowledge of the measured OSNR, and without the OSNR, respectively. The second method based on certain features of In-Phase and Quadrature histograms and with use of KNN reached up to 80% accuracy when information is OSNR is given, and 66% when the OSNR information is not known by receiver. Therefore, both methods could be used as monitoring tools to control lasers frequencies in future terabit gridless multicarrier systems.

Furthermore, KNN, *k*-Means and FCM algorithms were adapted for 16-QAM non-symetrical demodulation in a simulated coherent optical system. Algorithms were implemented in DSP-based coherent receiver, after LMS equalizer module. Results showed that KNN slightly increases the BER when launch power of 0 dBm. It is due to nonlinear effects of the optical fiber are not stimulated and the training data was chosen with symbols affected by nonlinear distortions. Whilst with launch power of 9 dBm, for 1 kHz and 25 kHz of laser linewidth, a gain up to 2 dB is obtained. The use of clustering techniques (*k*-Means and FCM), outperforms conventional demodulation in all cases, presenting both, same performance for all scenarios.

Besides, it is experimentally demonstrated the use of *k*-Means and KNN algorithms to minimize ICI impact in gridless Nyquist-WDM systems. The proposed methods improved conventional demodulation in all cases, achieving gains up to 0.7 dB at BER of 1×10^{-2}. The mitigation of ICI was the same by *k*-Means and KNN, and *k*-Means shown better performance when the channel overlapping was minimum. Thus, these demodulation techniques would be useful to be implemented in future elastic/flexible networks. Finally, computational complexity is an issue to be further explore by all the proposed methods.

7. References

[1] D. M. Marom *et al.*, "Survey of Photonic Switching Architectures and Technologies in Support of Spatially and Spectrally Flexible Optical Networking [Invited]," *J. Opt. Commun. Netw.*, vol. 9, no. 1, p. 1, 2016.

[2] International Telecommunication Union - ITU-T, "G.694.1 (06/2002), Spectral grids for WDM applications: DWDM frequency grid," *Ser. G.694.1*, p. 14, 2002.

[3] V. Vgenopoulou, N. P. Diamantopoulos, I. Roudas, and S. Sygletos, "MIMO Nonlinear Equalizer based on Inverse Volterra Series Transfer Function for Coherent SDM Systems," *2019 Opt. Fiber Commun. Conf. Exhib. OFC 2019 - Proc.*, vol. 1, no. Cd, pp. 1–3, 2019.

[4] L. Wang, F. Jiang, M. Chen, H. Dou, G. Gui, and H. Sari, "Interference Mitigation Based on Optimal Modes Selection Strategy and CMA-MIMO Equalization for OAM-MIMO Communications," *IEEE Access*, vol. 6, pp. 69850–69859, 2018.

[5] W. Wang *et al.*, "Demonstration of 6 × 10-Gb/s MIMO-Free Polarization- and Mode-Multiplexed Transmission," *IEEE Photonics Technol. Lett.*, vol. 30, no. 15, pp. 1372–1375, 2018.

[6] M. Sato, R. Maher, D. Lavery, K. Shi, B. C. Thomsen, and P. Bayvel, "Frequency diversity MIMO detection for DP-QAM transmission," *J. Light. Technol.*, vol. 33, no. 7, pp. 1388–1394, 2015.

[7] T. Koike-Akino *et al.*, “Han-Kobayashi and dirty-paper coding for superchannel optical communications,” *J. Light. Technol.*, vol. 33, no. 7, pp. 1292–1299, 2015.

[8] J. J. G. Torres, A. M. C. Soto, and N. G. González, “Enhanced intercarrier interference mitigation based on encoded bit-sequence distribution inside optical superchannels,” *Opt. Eng.*, vol. 55, no. 10, pp. 1–6, Oct. 2016.

[9] F. Alishahi *et al.*, “Optical mitigation of interchannel crosstalk for multiple spectrally overlapped 20-GBd QPSK/16-QAM WDM channels using nonlinear wave mixing,” *J. Light. Technol.*, vol. 37, no. 2, pp. 548–554, 2019.

[10] A. Mohajerin-Ariaei *et al.*, “Demonstration of Tunable Mitigation of Interchannel Interference of Spectrally Overlapped 16-QAM/QPSK Data Channels using Wave Mixing of Delayed Copies,” 2017, p. Th3J.5.

[11] P. Wright, A. Lord, and L. Velasco, “The network capacity benefits of flexgrid,” *Int. Conf. Opt. Netw. Des. Model.*, no. c, pp. 7–12, 2013.

[12] F. Zhang, Q. Zhuge, and D. V. Plant, “Fast analytical evaluation of fiber nonlinear noise variance in mesh optical networks,” *J. Opt. Commun. Netw.*, vol. 9, no. 4, pp. C88–C97, 2017.

[13] R. Dar, M. Feder, A. Mecozzi, and M. Shtaif, “Inter-channel nonlinear interference noise in WDM systems: Modeling and mitigation,” *J. Light. Technol.*, vol. 33, no. 5, pp. 1044–1053, 2015.

[14] P. Serena and A. Bononi, “An alternative approach to the gaussian noise model and its system implications,” *J. Light. Technol.*, vol. 31, no. 22, pp. 3489–3499, 2013.

[15] Z. Dong, F. N. Khan, Q. Sui, K. Zhong, C. Lu, and A. P. T. Lau, “Optical Performance Monitoring: A Review of Current and Future Technologies,” *J. Light. Technol.*, vol. 34, no. 2, pp. 525–543, 2016.

[16] F. N. Khan, C. Lu, and A. P. T. Lau, “Optical performance monitoring in fiber-optic networks enabled by machine learning techniques,” *2018 Opt. Fiber Commun. Conf. Expo. OFC 2018 - Proc.*, pp. 1–3, 2018.

[17] J. J. Granada Torres *et al.*, “Mitigation of time-varying distortions in Nyquist-WDM systems using machine learning,” *Opt. Fiber Technol.*, vol. 38, no. March, pp. 130–135, 2017.

[18] E. A. Fernandez, J. J. G. Torres, A. M. C. Soto, and N. G. González, “Demodulation of m-ary non-symmetrical constellations using clustering techniques in optical communication systems,” *2016 IEEE Lat. Am. Conf. Comput. Intell. LA-CCI 2016 - Proc.*, no. 53, pp. 0–5, 2017.

[19] D. Wang *et al.*, “Nonlinearity Mitigation Using a Machine Learning Detector Based on k -Nearest Neighbors,” *IEEE Photonics Technol. Lett.*, vol. 28, no. 19, pp. 2102–2105, 2016.

[20] S. Ma *et al.*, “Signal Demodulation with Machine Learning Methods for Physical Layer Visible Light Communications: Prototype Platform, Open Dataset, and Algorithms,” *IEEE Access*, vol. 7, no. c, pp. 30588–30598, 2019.

[21] J. Mata *et al.*, “Application of Artificial Intelligence Techniques in Optical Networks,” *IEEE Photonics Soc. Summer Top. Meet. Ser. SUM 2018*, pp. 23–24, 2018.

[22] Q. Zhuge and W. Hu, “Application of Machine Learning in Elastic Optical Networks,” *Eur. Conf. Opt. Commun. ECOC*, vol. 2018-Septe, no. 1, pp. 1–3, 2018.

[23] T. Tanimura, T. Hoshida, T. Kato, S. Watanabe, and H. Morikawa, “Convolutional neural network-based optical performance monitoring for optical transport networks,” *J. Opt. Commun. Netw.*, vol. 11, no. 1, pp. A52–A59, 2019.

[24] Q. Zhuge *et al.*, “Application of Machine Learning in Fiber Nonlinearity Modeling and Monitoring for Elastic Optical Networks,” *J. Light. Technol.*, vol. 37, no. 13, pp. 3055–3063, 2019.

[25] A. E. P and J. J. G. Torres, “KNN , k-Means and Fuzzy c-Means for 16-QAM Demodulation in Coherent Optical Systems,” no. 53, pp. 8–11, 2019.

[26] A. E. Pérez, J. J. G. Torres, and N. G. González, “KNN-based Demodulation in gridless Nyquist-WDM Systems affected by Interchannel Interference,” pp. 1–2, 2019.

[27] P. Del Moral and S. Penev, “Fuzzy clustering and data analysis toolbox,” *Stoch. Process.*, pp. 141–220, 2018.

[28] N. G. Gonzalez, D. Zibar, A. Caballero, and I. T. Monroy, “Experimental 2.5-gb/s qpsk wdm phase-modulated radio-over-fiber link with digital demodulation by a *k*-means algorithm,” *IEEE Photonics Technology Letters*, vol. 22, no. 5, pp. 335–337, 2010.